applied sciences

Review

Some Practical Acoustic Design and Typical Control Strategies for Multichannel Active Noise Control

Yijing Chu [1], Ming Wu [2], Hongling Sun [2], Jun Yang [2,*] and Mingyang Chen [1]

1 State Key Laboratory of Subtropical Building Science, South China University of Technology, Guangzhou 510641, China; chuyj@scut.edu.cn (Y.C.); chenmingyang208@gmail.com (M.C.)
2 Key Laboratory of Noise and Vibration Research, Institute of Acoustics, Beijing 100190, China; mingwu@mail.ioa.ac.cn (M.W.); hlsun@mail.ioa.ac.cn (H.S.)
* Correspondence: jyang@mail.ioa.ac.cn

Abstract: Active noise control (ANC) systems usually involve a large number of loudspeakers and error microphones in order to achieve noise reduction over an extended region of space. Although fundamentals of ANC theory and principles of ANC methods have been well-established over the past 40 years, applications of this technology are facing new challenges. A larger quiet zone with better noise reduction performance is always desirable in a variety of real-life scenarios. This paper presents several important factors that affect the performance of multichannel ANC systems in some popular applications such as windows with natural ventilation and quiet-zone around heads. The factors affecting acoustic design include the reflection of a baffle plate, arrangement of error sensors in open areas, and so on. In addition, different control strategies are compared and analyzed, including centralized, decentralized, and distributed strategies. All these strategies are discussed from the signal processing side, which should be considered after a proper acoustic design. One of the important aims of this paper is to provide practical guidance for acoustic design and discuss several typical control strategies for multichannel ANC systems.

Keywords: multichannel active noise control (ANC); acoustic design; signal processing

check for updates

Citation: Chu, Y.; Wu, M.; Sun, H.; Yang, J.; Chen, M. Some Practical Acoustic Design and Typical Control Strategies for Multichannel Active Noise Control. *Appl. Sci.* **2022**, *12*, 2244. https://doi.org/10.3390/app12042244

Academic Editor: Lamberto Tronchin

Received: 16 January 2022
Accepted: 17 February 2022
Published: 21 February 2022

1. Introduction

Active noise control (ANC) systems have been widely used in both industrial machinery and consumer products. Since noise control usually needs to be executed within an extended area, ANC systems use a number of error microphones and loudspeakers to monitor noise and generate anti-sound, thereby attenuating the unwanted sound propagation over a certain region rather than at several spots. The fundamentals of ANC theory and principles of ANC methods have been well-established over the last 40 years [1–3]. However, successful applications of the technology are still limited to some specific cases, such as headsets, earplugs, and ventilation ducts where the unwanted noise is reduced only at a single spot or within a certain "duct-like space" [4]. With the development in audio and digital signal processing (DSP) equipment [5], and market driving force, active control for noise has been pushed towards a direction where the acoustic field is controlled within an enlarged area such that a real "quiet zone" could be created.

Both the physical and signal processing aspects should be considered to generate a "quiet zone". As the first step, the physical design involves several distinct acoustic objectives and the associated optimization of the acoustic system [6–9]. The physical design determines the best possible performance that an ANC system can achieve. This best possible performance is called the performance upper limit of the ANC system. On the other hand, the control strategies and the corresponding ANC algorithms play a critical role in guaranteeing the ANC system to reach this performance upper limit. To achieve the optimum, the design process should go through both acoustic and algorithm optimization, conducting computer simulations, and finally implementing and testing a real-time controller to ensure its performance and robustness.

One of the main aims of this paper is to emphasize the importance of understanding the advantages that acoustic and methodology optimization can create for multichannel ANC systems and a better appreciation of limitations that multichannel ANC systems could have. To this end, we will first discuss in this paper several acoustic design methods for multichannel ANC systems over the last decade, each of which aims to provide practical guidance for the physical design in some popular applications. The multichannel control strategies that use different optimization principles for signal processing are then reviewed and compared. These control strategies include the centralized, decentralized, and diffusion optimization methods. All the studies discussed here are application-oriented, e.g., preventing sound transmission from building openings and compact noise sources, or generating a quiet-zone around heads.

2. Practical Acoustic Design

2.1. Effect of Reflecting Surface on ANC

Compared to the free-field control, the noise control in an enclosure is somewhat more difficult due to the reflecting surfaces that may cause complicated acoustic mode distribution [10]. A lot of research has been carried out to understand the effects of reflecting surfaces physically [11,12]. In a recent study [13], it was found that introducing a reflecting surface could increase sound pressure generated by the secondary sources such that the noise reduction performance is improved. It also found that the beneficial frequency range extends with the number of channels of the control system. In addition, the upper limit frequency range is determined by the distance between the secondary sources and the location of the secondary sources around the primary source. It indicated that the multichannel system may have a better performance than the single channel one in terms of both the controllable area and the frequency range.

Table 1 shows the simulation results in Tao's 2017 paper [13]. The cross frequency and the optimal noise reduction (NR) at a frequency of 800 Hz are listed. The NR results in both the free space and a half space with a reflecting surface are compared. The cross frequency is defined as the minimal frequency that the optimal noise reduction of the system with a reflecting surface equals to that in free field. The higher the cross frequency is, the wider the controllable frequency range becomes. It can be seen that the improvement of the optimal noise reduction by introducing a reflecting surface increases with the number of channels of ANC systems.

Table 1. Simulation results for the cross frequency and the optimal noise reduction at 800 Hz using 2-channel, 3-channel, and 4-channel ANC systems in Tao's 2017 paper [13].

Channel Number	2-Channel	3-Channel	4-Channel
Cross frequency (Hz)	970	1180	1280
Optimal NR in free space (dB)	4.7	8.5	10
Optimal NR with a reflecting surface (dB)	6.4	17.0	28
Improvement of the optimal NR (dB)	1.7	8.5	18

In [13], experiments were also conducted in an anechoic chamber as shown in Figure 1. A wooden plate is used as the reflecting surface. ANC systems with different numbers of loudspeakers and error microphones were tested. The primary source was placed in the center of the half-circle frames. In Figure 1a, the wooden plate was mounted and five error microphones in total were placed on the half-circle frames. In Figure 1b, the free field was considered and five more error microphones were used. The loudspeakers that work as the secondary sources of the multichannel ANC system were mounted on a small adjustable frame as shown in Figure 1c,d. The experimental and simulated optimal NR results are compared in Figure 2. The results verify that the noise reduction can be improved by introducing the reflecting surface and the improvement is more significant if more channels are used.

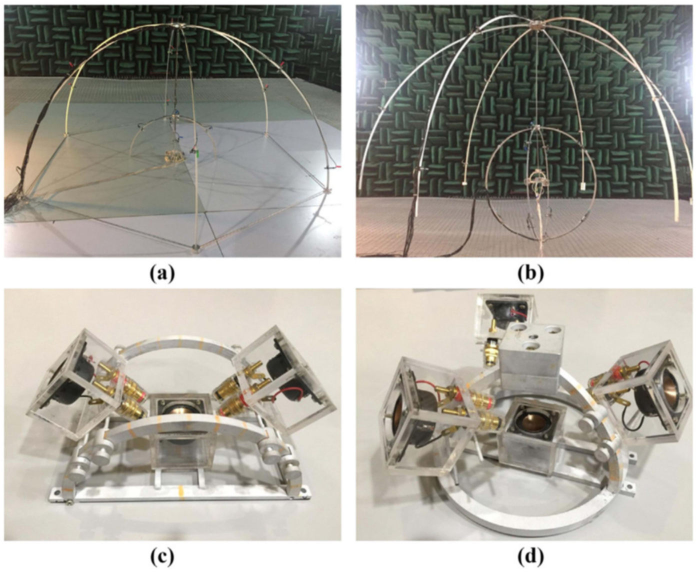

Figure 1. Experimental setup in Tao's 2017 paper [13]: (**a**) a 3-channel ANC system setup with a wooden plate as the reflecting surface; (**b**) a 3-channel ANC system setup in free field; (**c**) a configuration of a 2-channel ANC system; (**d**) a configuration of a 3-channel ANC system.

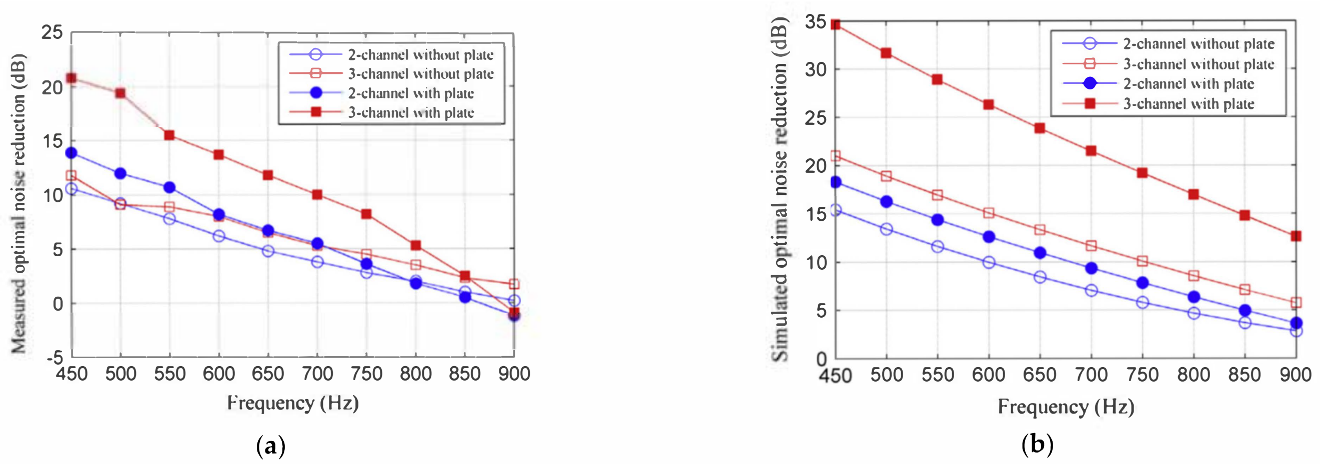

Figure 2. Optimal noise reduction with and without the wooden plate (**a**) measured results (**b**) simulation results. Figures are cited from Tao's 2017 paper [13].

2.2. ANC in Open Areas around Head

In a lot of applications, the multichannel ANC system either has to generate a quiet zone surrounding a human's head [14,15] or prevent the noise radiation from a compact noise source [16]. A well-designed 16-channel cylindrical ANC system has been proposed to generate a "quiet zone" within an area as large as a human head [17,18]. The diffraction of the head and locations of the error microphones and loudspeakers affect the performance of such systems significantly. In [17], the effect of a diffracting sphere on this system was studied. As shown in Figure 3a (cited from Zou's 2008 paper [17]), experiments were carried out in an irregular room of about 80 m^3. The primary noise sources were located in three different directions and generated by the same amplified pure-tone signal. Sixteen speakers and sixteen microphones, distributed on two layers, were used as control sources and error sensors, respectively. The filtered-x algorithm was used to generate the anti-sound of the 16-channel ANC system. To study the effect of the human head on the control performance, a hollow iron sphere of a radius about 0.09 m was used to approximate the human head. The experimental results show that the NR can be improved by the diffracting sphere, especially in higher frequency as shown in Figure 3b.

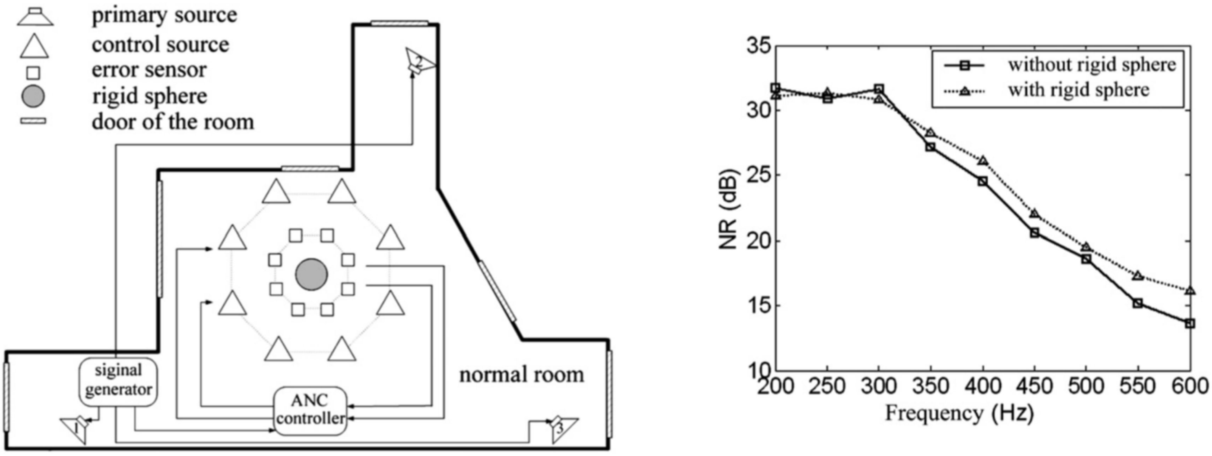

(**a**) (**b**)

Figure 3. (**a**) Experimental setup; (**b**) experimental result of the control performance with or without a sphere. Figures are cited from Zou's 2008 paper [17].

In a similar experiment reported in [18] where the diffracting sphere is not considered, it was shown that a larger radius of error sensors (a_e) may cause noise reduction to decrease, as shown in Figure 4a (cited from Zou's 2007 paper [18]). It also reported that the control performance improves rapidly with an increase in the radius of controllers (a_c) if a_c is close to a_e, indicating that secondary sources should not be too close to error sensors as shown in Figure 4b from [18]. As explained in [18], the main reason is that when the loudspeaker is close to one of the error sensors, the contribution of the anti-sound is dominated by the closest loudspeaker only. In this way, a global optimization is hardly achieved. As the distance increases to a certain value, the control sources affect the entire cylindrical surface and the noise control is more efficient.

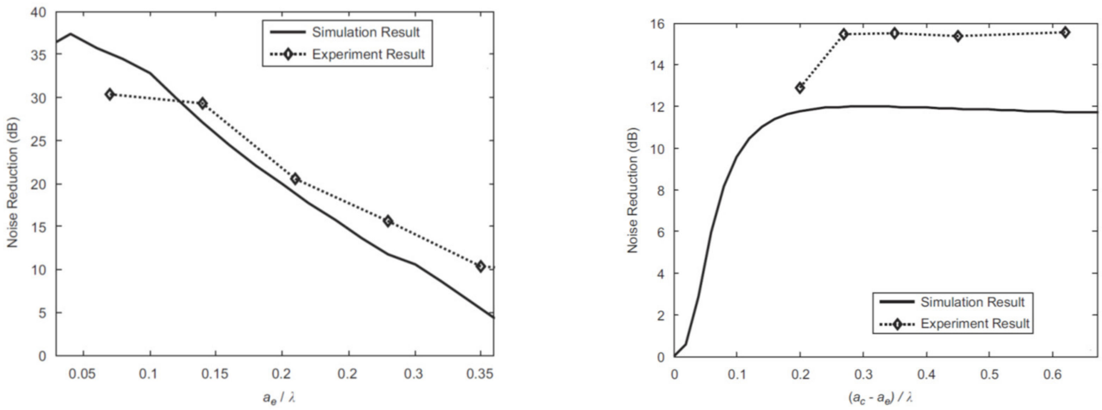

(**a**) (**b**)

Figure 4. Control performance (**a**) with respect to a_e, f = 250 Hz, a_c = 1.22 m; (**b**) with respect to a_c–a_e, f = 250 Hz, a_e = 0.38 m. Figures are cited from Zou's 2007 paper [18].

2.3. ANC in the Opening of Buildings

Another problem that is worthy of study is the noise control at openings of an enclosure [19–26]. It has been found that more error sensors usually produce a better noise control performance. In [23], a multichannel ANC system designed for a window with natural ventilation is proposed. This system was tested on a full-size window, where 16 control channels are evenly distributed across the window opening. It showed that the window installed with this ANC system could attenuate noise as effectively as the fully-glazed window while natural ventilation is still maintained.

In another study [24], a boundary arrangement of error microphones was investigated. Compared to the abovementioned distributed arrangement [23], the boundary arrangement allows better natural ventilation and lighting. It was found that a double-layer error microphone arrangement over the boundary could achieve a better performance than a single-layer one. The experiments were carried out in an anechoic chamber. A cabinet with an opening was used as a room model with a window. The opening was embedded on a baffle as shown in Figure 5a. An ANC system with 32 channels was mounted in the room model. Three configurations of error microphones were used, i.e., evenly distributed, single-layer, and double-layer as shown in Figure 5b–d. There are some interesting findings in the experiments and computer simulations with the same setting. The performance is summarized in Table 2. First, it was found from computer simulations that the upper-limit frequency of the enclosure could be increased by adding more layers of error microphones at the edge. Secondly, the double layer strategy had higher NR than that of the single layer one. This conclusion provides useful guidance for ANC acoustic arrangement.

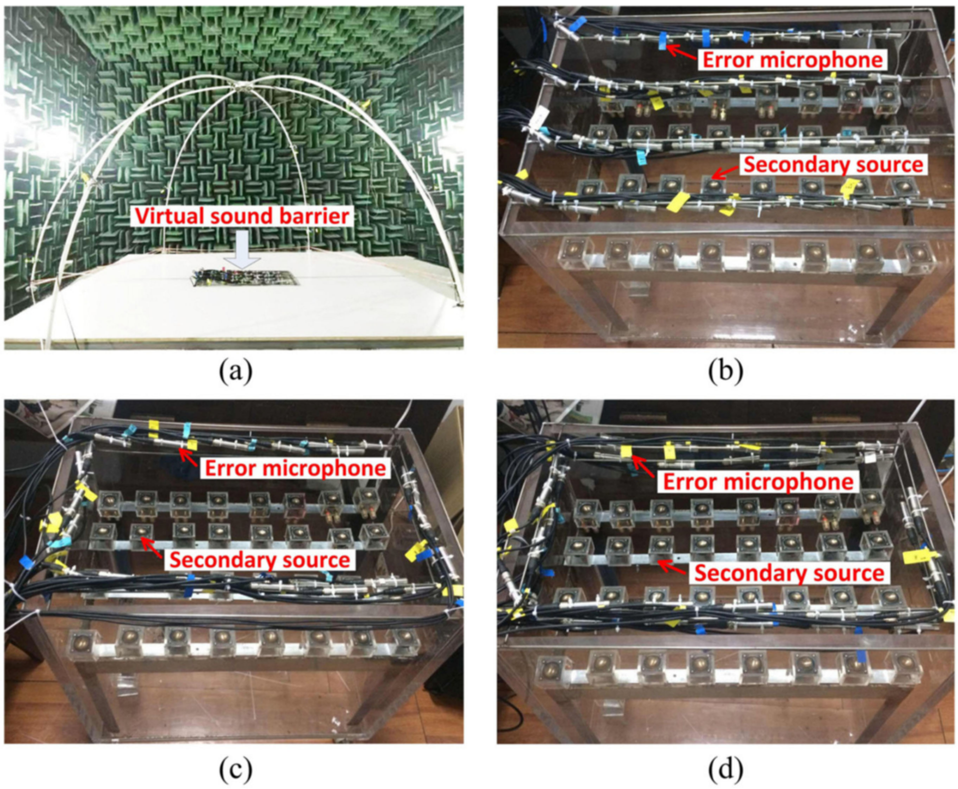

Figure 5. (Color online) Photos of the experiment setup: (**a**) a panoramic view of the anechoic chamber, (**b**) evenly distributed error microphones, (**c**) single layer error microphones at the edge, and (**d**) double-layer error microphones at the edge. Figures are cited from Wang's 2019 paper [24].

Table 2. Performance Comparison of Three Error Microphone Distributions.

	Evenly Distributed	Single-Layer	Double-Layer
Upper-Limit Frequency (simulation)	-	Low	High
Averaged NR from 500 to 1000 Hz (experiments)	High	Low	Medium
Ventilation and lighting	Good	Better than distributed arrangement	

3. Three Active Control Strategies

Given a certain acoustic design, the control algorithm determines the final performance of an ANC system. A lot of ANC algorithms have been developed. For example, in Zou's papers [17,18], each of the 16 controllers use the filtered-x least mean squares (FxLMS) algorithm [27] to generate proper anti-sound. In Tao's 2017 paper [13], a commercial ANC system, namely Antysound Tiger ANC-II, was used for noise control.

To make the multichannel controllers cooperate with each other, different strategies could be employed. In this subsection, three frequently used control strategies, i.e., the centralized, decentralized, and distributed strategies, are discussed. The properties of the three strategies are briefly summarized in Table 3. First, we compare these strategies in terms of the structure (see Figure 6) and the computational complexity (see Table 4). Then, we report recent progress in the decentralized and distributed control strategies that consume less hardware resources and are much easier to be implemented in real applications.

Table 3. Brief Summary of Various Control Strategies.

	Centralized FxLMS	Decentralized FxLMS	Distributed FxLMS
Cost function	$J_c = E[\sum_{k=1}^{K} e_k^2(n)]$	$J_{d\_k} = E[e_k^2(n)]$ for $k = 1, \ldots, K$	$J_{dis\_k} = E[e_k^2(n)]$ $s.t.\ w_k = w_l, l \in N_k / \{k\}$ for $k = 1, \ldots, K$
Performance in general cases	High	Low	Close to centralized FxLMS
Complexity	High	Low	Low

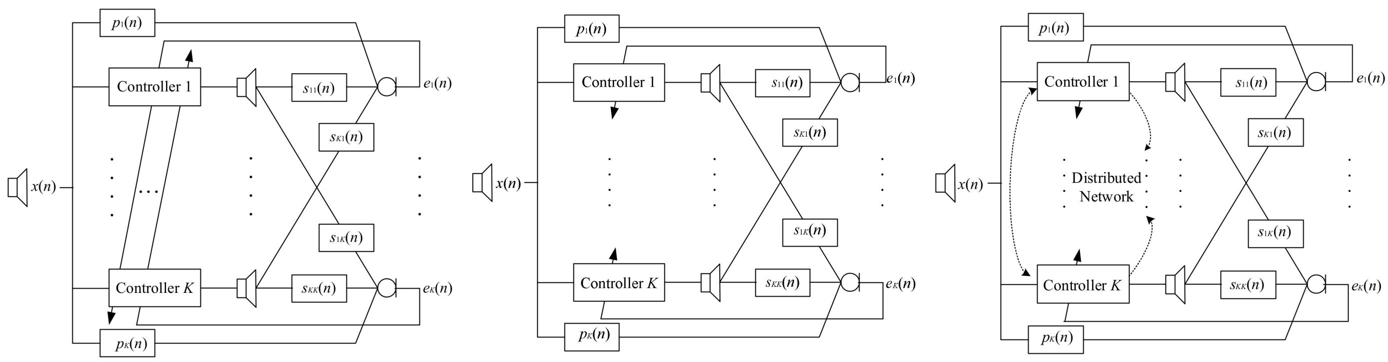

Figure 6. Cost functions and block diagrams of ANC systems with different control strategies: (**a**) centralized; (**b**) decentralized; and (**c**) distributed.

Table 4. Arithmetic Complexities of Various Control Methods.

	Centralized FxLMS	Decentralized FxLMS	Distributed FxLMS
Secondary path modeling	K^2	K	K
Adaptive filter	K^2L	KL	KL

The centralized control was first proposed as the multiple error (ME) ANC algorithm in Elliott's 1987 paper [28]. The MEANC algorithm could also be implemented by FxLMS or its variants [29–32] if the noise signal, known as reference signal, is collected. MEANC optimizes the residue over all channels such that each controller updates the coefficients by using data from all error microphones (see the cost function in Table 3 and diagram for the centralized ANC system with K loudspeakers/error microphones in Figure 6a).

Different from the centralized control, the decentralized control [33] lets each controller minimize the error power at one error microphone only (see the cost function in Table 3 and diagram in Figure 6b). Comparing Figure 6a,b, it can be seen that, the centralized controller needs to process signals from all the error microphones and model K^2 transfer functions while the decentralized controller only processes signals from one error microphone. Therefore, the decentralized structure could decrease the computational burden from order K^2 to K. The computational complexity of these two structures are compared in Table 4.

To balance between the complexity and overall performance, a third structure, called the distributed control, has been developed in the recent 5 years. From the cost function of the diffusion control shown in Table 3 and its diagram in Figure 6c, it can be seen that the distributed strategy also processes signals from one error microphone such that it has a complexity comparable to the decentralized strategy (see Table 4). It further combines the controller parameters along a linking path or within a neighborhood N_k for $k = 1, ..., K$ according to the incremental [34] or diffusion [35] rule, which could increase the system robustness without involving any extra multiplication.

Since the three control strategies use different noise control principles, it turns out that the centralized processing that optimizes the global error generally outperforms the decentralized one that deals with the local error. The decentralized noise control needs properly selected diagonal loading to balance between stability and control accuracy. It has also been noticed that the centralized control shows little improvement over the decentralized one if both are limited to the same control effort [36]. The distributed control optimizes the local error at each channel subject to a set of constraints that reject large values of the controller coefficients. Therefore, it usually has a better robustness than the decentralized control due to the spatial constrains ($w_k = w_l$) it employs. A brief summary of the three strategies in terms of the performance and computational cost is listed in Tables 3 and 4. It can be seen that, generally, the distributed strategy has a performance close to the well-performed centralized one and a computational complexity as low as the hardware-efficient decentralized control. A comparison of the three strategies as well as a detailed performance analysis of the distributed strategy will be presented in Sections 3.1 and 3.2.

3.1. Decentralized Control

Due to the reduced complexity and better feasibility for hardware implementation of multi-channel control systems, the decentralized control technique has been widely used [37–45]. To compensate the performance loss, a recent research proposed a method that properly chooses a so-called eigenvalue matrix so that a two-channel decentralized ANC system achieves the same noise reduction performance as the centralized one with guaranteed convergence [44].

A comparison of several conventional control strategies has been conducted by computer simulations (see Figure 7 cited from Zhang's 2019 paper [44]). It seems that the proposed eigenvalue selection method is equivalent to constantly changing the step-sizes of the two channels since the multiplication of the step-size and the eigenvalue matrix, which is a diagonal matrix for two-channel systems, determines the total update of the ANC algorithm. The decentralized control strategy could be generalized to a system with more channels and different gradient searching methods [40].

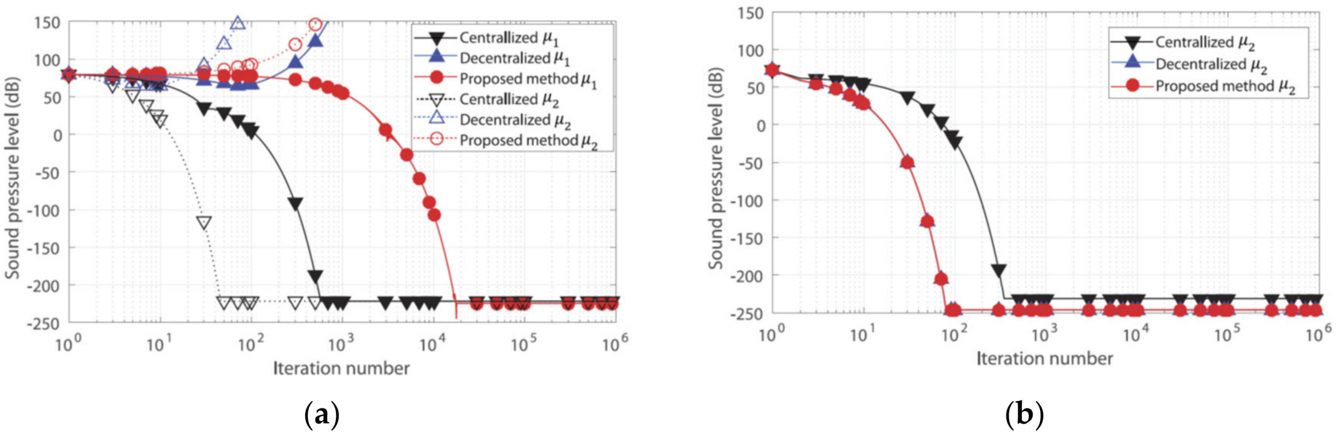

Figure 7. Convergence curves of the three methods with weighting factors of zero at (**a**) 130 Hz and (**b**) 200 Hz, where the step-sizes $\mu_1 = 1 \times 10^{-7}$ and $\mu_2 = 1 \times 10^{-6}$. Figures are cited from Zhang's 2019 paper [44].

Experiments using a decentralized active control system to reduce the vibration of a plate have been carried out in [43]. To compensate the instability caused by decentralized structure, a digital phase lag compensator has been designed. In this way, the eigenvalue of the open loop transfer function matrix could be managed so as to guarantee the stability of the multichannel decentralized system. The control system is mounted on a panel–cavity system as shown in Figure 8. At the corner of the cavity, there is a loudspeaker to generate the primary disturbance. Based on this experimental facility, the control performance of the proposed decentralized control system with different numbers of control loops are investigated. The total kinetic energy of the plate between 1 and 1 kHz has been used as a measure of the vibration reduction. The results for, respectively, two and nine control loops are presented in Figure 9. Generally, greater reduction can be achieved by nine control loops. This is because the control units distributed at the edges of the plate can effectively reduce the vibration of the corresponding mode.

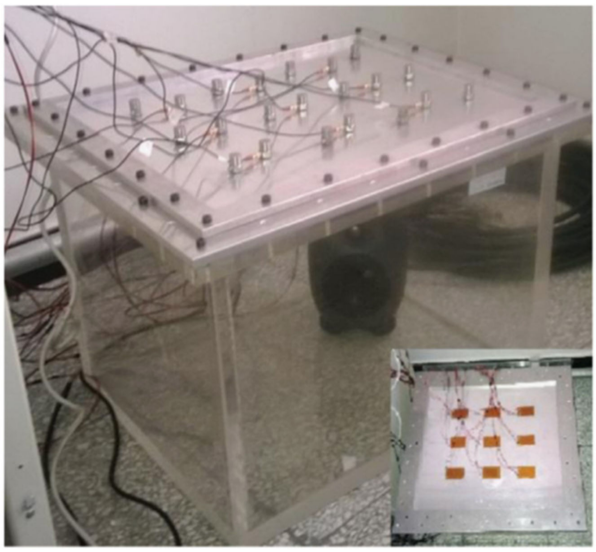

Figure 8. The experimental facility of a panel–cavity system: aluminum panel with error sensors and nine collocated sensor–actuator pairs. Figure is cited from Yu's 2015 paper [43].

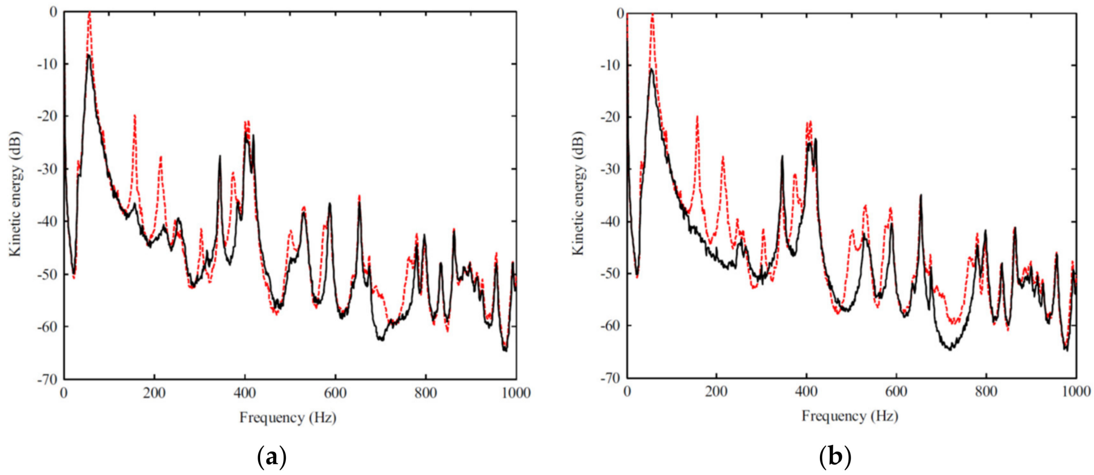

Figure 9. The kinetic energy of the plate with the excitation of the loudspeaker in the cavity between 1 and 1 k Hz without control (dashed line), and when the two control loops (**a**), nine control loops (**b**) are implemented (solid line). Figures are cited from Yu's 2015 paper [43].

3.2. Distributed Control

The distributed noise control is a technique that was developed in the recent 5 years [35]. Several different linking networks have been adopted in ANC algorithms. An incrementally collaborative structure [46] was first used in ANC systems. As shown in Figure 10, each node represents an ANC controller for a channel and the distributed structure allows communication between different controllers (see Figure 6c). It was found that the distributed structure is more robust than the decentralized ANC algorithm [35]. The incremental control shown in Figure 10a, however, suffers from several drawbacks for real-time adaptation over networks, such as the sensitivity to the failure of a single node, the limited data communication between nodes, and the fixed simple cyclic path for incremental steps. To overcome these problems, the diffusion strategy [47], as shown in Figure 10b, has been developed.

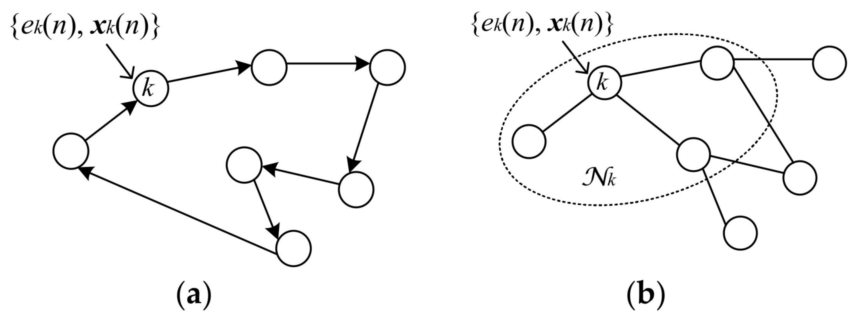

Figure 10. Distributed network of node k: (**a**) an incremental structure where nodes update along a cyclic loop, and (**b**) a diffusion structure where nodes communicate within a neighborhood N_k. Node k collects the residue and reference data set $\{e_k(n), \boldsymbol{x}_k(n)\}$ at time index n.

New diffusion MEFx-like ANC algorithms have been proposed recently [36,48]. In [48], the convergence behavior of the diffusion FxLMS (Diff-FxLMS) algorithm was investigated. The mean and mean squares difference equations for the adaptive process were derived, based on which the convergence curves and conditions, and the steady-state solutions were obtained. In the mean performance analysis, it was found that the combining strategy brings in an estimation bias to the Wiener solution of the controller. The estimation bias is caused by the difference in the primary and secondary paths at different channels (the primary path represents the acoustic response from the noise source to the error microphone while the secondary path represents the response from the anti-sound loudspeaker to the error microphone). Specifically, since the primary and secondary paths are different, the optimal solutions to controllers at each channel are also different. When the diffusion strategy is applied and combines the local estimates at each channel, the spatial averaging brings in an estimation bias.

To quantify such an estimation bias, both theoretical analysis and simulations are carried out. It is assumed that the primary paths p_i are randomly distributed on a circle of radius r centered at p_0, i.e., $p_i = p_0 + rg_i$, for $i = 1, 2, \ldots$, and g_i is a Gaussian sequence of unit norm. Figure 11 examines whether the controllers converge to the Wiener solution or the theoretical steady-state solution derived in [48]. The curves show that the deviation of the estimate to the Wiener solution (denoted as v^0 in the Figure) is larger than that to the theoretical steady-state solution (denoted as v^{inf} in the Figure). Therefore, an increased bias will be observed in diffusion ANC systems.

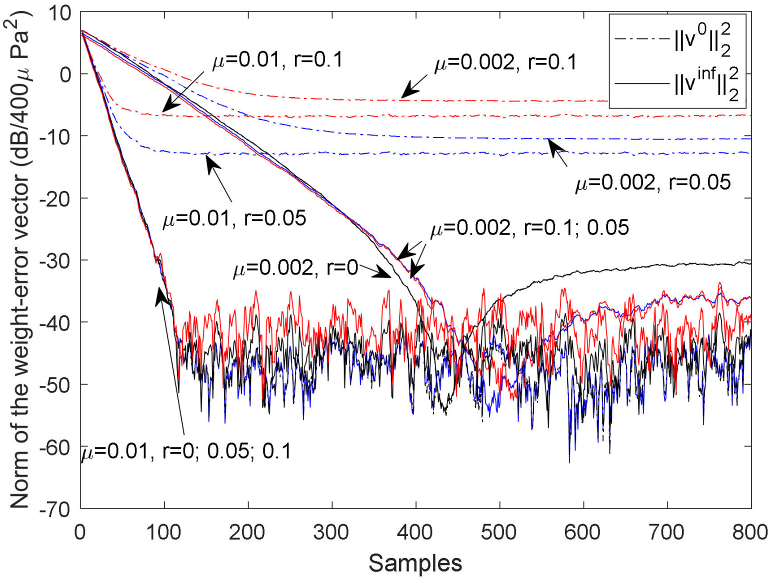

Figure 11. Learning curves of the norm of the estimate deviation to the Wiener solution v^0 and the deviation to the theoretical steady-state solution v^{inf} under different settings. The number of node $K = 10$. μ and r are, respectively, the step-size and the radius that controls the difference between the primary paths. Figure is cited from Chu's 2020 paper [48].

The theoretical analysis of the mean squares performance of the Diff-FxLMS is further verified in Figure 12. Generally, the theoretical and simulated global excess mean square error (EMSE) curves agree well with each other under different settings of step-sizes μ and radius r. It also shows that as the value of r increases, i.e., the optimal solution to each node becomes more different from each other, the steady-state EMSE becomes larger. Finally, three different multichannel strategies are compared in Figure 13. To have a reasonable comparison, the step-sizes are set to be identical. It shows that the incremental control method has a higher steady-state residual noise level while the decentralized control method increases the EMSE value gradually as the iteration. The diffusion control has a similar performance as the well-performed centralized control. It shows that, compared to the decentralized control, the diffusion strategy brings in a better robustness via the spatial regularization. It can be explained by the constraint $w_k = w_l$ that requires the nearby controllers within a neighborhood to stay close to each other.

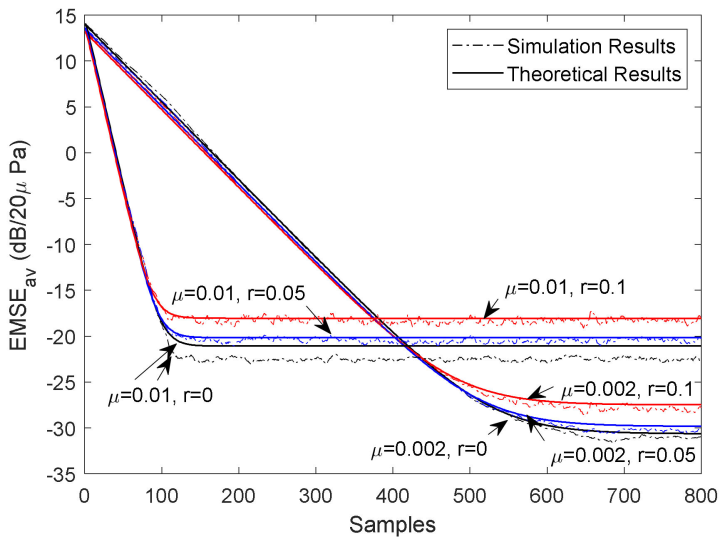

Figure 12. Learning curves of averaged global EMSE under different settings. $K = 10$. Figure is cited from Chu's 2020 paper [48].

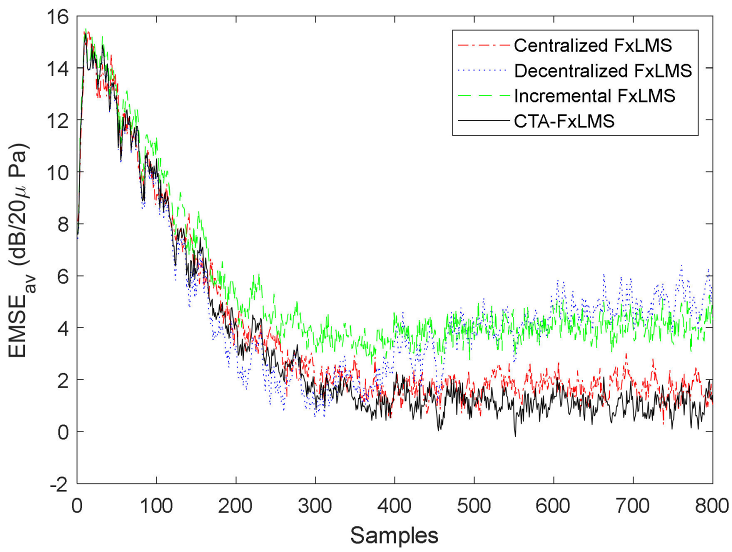

Figure 13. Global EMSE learning curves with different control strategies for the ANC controller: $\mu = 0.001$, $r = 0.01$, $K = 10$ and the filter length $L = 160$. Figure is cited from Chu's 2020 paper [48].

4. Conclusions

This paper discusses several problems in multichannel ANC systems that researchers or technicians working in real applications often meet. We aim to provide a guidance for ANC system design, which involves both acoustic and signal processing efforts. Findings from the acoustic side indicate that diffracting surface and more channels with a proper physical distribution may increase the noise control performance in terms of the controllable frequency range and noise reduction. As the size of the multichannel ANC system increases, the control strategy and algorithms play a more important role in the final control performance. Based on a chosen control strategy, adaptive networks and filtering techniques, such as the leaky, transform domain, and fast algorithms [31,49], could achieve a faster, more feasible, and more robust realization of noise control. These techniques are generally available to both single and multiple channel ANC systems. Interested readers can refer to the related papers. Applying the advanced acoustic design and signal processing techniques to commercial products is the trend for multiple channel ANC. Combining modern ANC technology with daily necessities such as headphones, head cushions, and so on will be performed in both academic and industry.

Author Contributions: Literature review and writing—original draft preparation, Y.C.; writing—revising and editing, M.W. and H.S.; funding acquisition, J.Y.; writing—editing, M.C. All authors have read and agreed to the published version of the manuscript.

Funding: The work described in this study was supported by Frontier Exploration Project Independently Deployed by Institute of Acoustics, Chinese Academy of Sciences (QYTS202009), National Natural Science Foundation of China (61901174), Guangdong Basic and Applied Basic Research Foundation (2019A1515010771), and the State Key Laboratory of Mechanical System and Vibration (Grant No. MSV202202).

Institutional Review Board Statement: Not applicable.

Informed Consent Statement: Not applicable.

Data Availability Statement: Not applicable.

Conflicts of Interest: The authors declare no conflict of interest. The funders had no role in the design of the study; in the collection, analyses, or interpretation of data; in the writing of the manuscript, or in the decision to publish the results.

References

1. Nelson, P.A.; Elliott, S.J. *Active Control of Sound*; Academic Press: Cambridge, MA, USA, 1992.
2. Kuo, S.M.; Morgan, D.R. *Active Noise Control Systems: Algorithms and DSP Implementations*; John Wiley & Son Inc.: Hoboken, NJ, USA, 1996.
3. Hansen, C.H.; Snyder, S.D.; Qiu, X.; Brooks, L.; Moreau, D. *Active Control of Noise and Vibration*, 2nd ed.; CRC Press: London, UK, 2013.
4. Bai, M.R.; Chen, H.Y.; Yang, L.H.; Huang, S.C. Active control of noise in a duct using the sparsely coded time-domain underdetermined multichannel inverse filters. *J. Acoust. Soc. Am.* **2019**, *146*, 1371–1381. [CrossRef] [PubMed]
5. An, F.; Sun, H.; Li, X. Adaptive active control of periodic vibration using maglev actuators. *J. Sound Vib.* **2012**, *331*, 1971–1984. [CrossRef]
6. Elliott, S.J.; Nelson, P.A. Active noise control. *IEEE Signal Process. Mag.* **1993**, *10*, 12–35. [CrossRef]
7. Cao, Y.; Sun, H.; An, F.; Li, X. Active control of low-frequency sound radiation by cylindrical shell with piezoelectric stack force actuators. *J. Sound Vib.* **2012**, *331*, 2471–2484. [CrossRef]
8. Wang, H.; Sun, H.; Sun, Y.; Wu, M.; Yang, J.; Li, X. A multi-tone active noise control system with a simplified local on-line secondary-path modeling. *J. Acoust. Soc. Am.* **2018**, *144*, EL515–EL521. [CrossRef]
9. Wang, H.; Sun, H.; Sun, Y.; Wu, M.; Yang, J. A narrowband active noise control system with a frequency estimation algorithm based on parallel adaptive notch filter. *Signal Process.* **2019**, *154*, 108–119. [CrossRef]
10. Ingard, U.; Lamb, G.L. Effect of a reflecting plane on the power output of sound sources. *J. Acoust. Soc. Am.* **1957**, *29*, 743–744. [CrossRef]
11. Pan, J.; Qiu, X.; Paurobally, R. Effect of reflecting surfaces on the performance of active noise control. In Proceedings of the ACOUSTICS, Christchurch, New Zealand, 20–22 November 2006.
12. Garcia-Bonito, J.; Elliott, S.J.; Bonilha, M. Active cancellation of pressure at a point in a pure tone diffracted diffuse sound field. *J. Sound Vib.* **1997**, *201*, 43–65. [CrossRef]
13. Tao, J.; Wang, S.; Qiu, X.; Pan, J. Performance of a multichannel active sound radiation control system near a reflecting surface. *Appl. Acoust.* **2017**, *123*, 1–8. [CrossRef]
14. Garcia-Bonito, J.; Elliot, S.J. Local active control diffracted diffuse sound fields. *J. Acoust. Soc. Am.* **1995**, *98*, 1017–1024. [CrossRef]
15. Duda, R.O.; Martens, W.L. Range dependence of the response of a spherical head model. *J. Acoust. Soc. Am.* **1998**, *104*, 3048–3058. [CrossRef]
16. Tao, J.; Guo, Q.; Qiu, X. A near-field error sensing strategy for compact multi-channel active sound radiation control in free field. *J. Acoust. Soc. Am.* **2019**, *145*, 2179–2187. [CrossRef]
17. Zou, H.; Qiu, X. Performance analysis of the virtual sound barrier system with a diffracting sphere. *Appl. Acoust.* **2008**, *69*, 875–883. [CrossRef]
18. Zou, H.; Qiu, X.; Lu, J.; Niu, F. A preliminary experimental study on virtual sound barrier system. *J. Sound Vib.* **2007**, *307*, 379–385. [CrossRef]
19. Field, C.D.; Fricke, F.R. Theory and applications of quarter-wave resonators: A prelude to their use for attenuating noise entering buildings through ventilation openings. *Appl. Acoust.* **1998**, *53*, 117–132. [CrossRef]
20. Parkins, J.; Sommerfeldt, S.; Tichy, J. Narrowband and broadband active control in an enclosure using the acoustic energy density. *J. Acoust. Soc. Am.* **2000**, *108*, 192–203. [CrossRef]

21. Wang, S.; Tao, J.; Qiu, X. Performance of a planar virtual sound barrier at the baffled opening of a rectangular cavity. *J. Acoust. Soc. Am.* **2015**, *138*, 2836–2847. [CrossRef]
22. Wang, S.; Tao, J.; Qiu, X.; Pan, J. Mechanisms of active control of sound radiation from an opening with boundary installed secondary sources. *J. Acoust. Soc. Am.* **2018**, *143*, 3345–3351. [CrossRef]
23. Lam, B.S.; Chuang, S.D.; Gan, W.S. Active control of sound through full-sized open windows. *Build. Environ.* **2018**, *141*, 16–27. [CrossRef]
24. Wang, S.; Tao, J.; Qiu, X.; Pan, J. A boundary error sensing arrangement for virtual sound barriers to reduce noise radiation through openings. *J. Acoust. Soc. Am.* **2019**, *145*, 3695–3702. [CrossRef]
25. Shi, D.Y.; Gan, W.S.; Lam, B.; Hasegawa, R.; Kajikawa, Y. Feedforward multichannel virtual-sensing active control of noise through an aperture: Analysis on causality and sensor-actuator constraints. *J. Acoust. Soc. Am.* **2020**, *147*, 32–48. [CrossRef]
26. Zhang, C.X.; Qin, M.; Zou, H.S.; Qiu, X.J. Secondary source and error sensing strategies for the active control of sound transmission through a small opening. *J. Sound Vib.* **2020**, *464*, 114973. [CrossRef]
27. Morgan, D.R. An analysis of multiple correlation cancellation loops with a filter in the auxiliary path. *IEEE Trans. Acoust. Speech Signal Process.* **1980**, *28*, 454–467. [CrossRef]
28. Elliott, S.; Stothers, I.; Nelson, P. A multiple error LMS algorithm and its application to the active control of sound and vibration. *IEEE Trans. Speech Signal Process.* **1987**, *35*, 1423–1434. [CrossRef]
29. Li, Y.; He, L.; Shuai, C.; Wang, F. Time-domain filtered-x-Newton narrowband algorithms for active isolation of frequency-fluctuating vibration. *J. Sound Vib.* **2016**, *367*, 1–21. [CrossRef]
30. Wu, L.; Qiu, X.; Burnett, I.S.; Guo, Y. A recursive least square algorithm for active control of mixed noise. *J. Sound Vib.* **2015**, *339*, 1–10. [CrossRef]
31. Tang, X.L.; Lee, C.M. Time–frequency-domain filtered-x LMS algorithm for active noise control. *J. Sound Vib.* **2012**, *331*, 5002–5011. [CrossRef]
32. Wu, M. An overlap-save frequency-domain implementation of the delayless subband ANC algorithm. *IEEE Trans. Audio Speech Lang. Process.* **2008**, *16*, 1706–1710. [CrossRef]
33. Elliott, S.J.; Boucher, C.C. Interaction between multiple feedforward active control systems. *IEEE Trans. Speech Audio Process.* **1994**, *2*, 521–530. [CrossRef]
34. Ferrer, M.; Diego, M.; Pinero, G.; Gonzalez, A. Active noise control over adaptive distributed networks. *Signal Process.* **2015**, *107*, 82–95. [CrossRef]
35. Ferrer, M.; Gonzalez, A.; de Diego, M.; Piñero, G. Distributed affine projection algorithm over acoustically coupled sensor networks. *IEEE Trans. Signal Process.* **2017**, *65*, 6423–6434. [CrossRef]
36. Engels, W.P.; Baumann, O.N.; Elliott, S.J. Centralized and decentralized control of structural vibration and sound radiation. *J. Acoust. Soc. Am.* **2006**, *119*, 1487–1495. [CrossRef]
37. Leboucher, E.; Micheau, P.; Berry, A.; L'Esperance, A. A stability analysis of a decentralized adaptive feedback active control system of a sinusoidal sound in free space. *J. Acoust. Soc. Am.* **2002**, *111*, 189–199. [CrossRef] [PubMed]
38. Baumann, O.N.; Elliott, S.J.; Berry, A. The stability of decentralized multichannel velocity feedback controllers using inertial actuators. *J. Acoust. Soc. Am.* **2002**, *111*, 189–199. [CrossRef]
39. Zhang, L.; Tao, J.; Qiu, X. Performance analysis of decentralized multi-channel feedback systems for active noise control in free space. *Appl. Acoust.* **2013**, *74*, 181–188. [CrossRef]
40. An, F.; Sun, H.; Li, X.; Tian, J. Optimization of parameters in decentralized adaptive active control algorithm. *J. Vib. Eng.* **2013**, *26*, 48–54.
41. Cao, Y.; Sun, H.; An, F.; Li, X. Virtual absorbed energy in decentralized velocity feedback control of a plate with piezoelectric patch actuators. *Appl. Acoust.* **2013**, *74*, 909–919. [CrossRef]
42. Cao, Y.; Sun, H.; Li, X. A novel decentralized feedforward control strategy for a plate vibration without secondary path modeling using piezo electric patch actuator. *J. Vib. Shock* **2014**, *33*, 98–104.
43. Yu, Y.; Sun, H.; Cao, Y.; An, F.; Yang, J. Experimental validation of virtual absorbed energy of piezoelectric patch actuators in decentralized velocity feedback control of a plate. *J. Sound Vib.* **2015**, *341*, 1–15. [CrossRef]
44. Zhang, G.; Tao, J.; Qiu, X.; Burnett, I. Decentralized Two-Channel Active Noise Control for Single Frequency by Shaping Matrix Eigenvalues. *IEEE/ACM Trans. Audio Speech Lang. Process.* **2019**, *27*, 44–52. [CrossRef]
45. Wang, K.; Tao, J.; Qiu, X. A time domain decentralized algorithm for two channel active noise control. *J. Acoust. Soc. Am.* **2020**, *147*, 3808–3813.
46. Lopes, C.; Sayed, A. Incremental adaptive strategies over distributed networks. *IEEE Trans. Signal Process.* **2007**, *55*, 4064–4077. [CrossRef]
47. Lopes, C.; Sayed, A. Diffusion least-mean squares over adaptive networks: Formulation and performance analysis. *IEEE Trans. Signal Process.* **2008**, *56*, 3122–3136. [CrossRef]
48. Chu, Y.J.; Mak, C.M.; Zhao, Y.; Chan, S.C.; Wu, M. Performance analysis of a diffusion control method for ANC systems and the network design. *J. Sound Vib.* **2020**, *475*, 1–17. [CrossRef]
49. Wu, L.F.; Qiu, X.J.; Guo, Y.C.; Chan, S.C.; Wu, M. A generalized leaky FxLMS algorithm for tuning the waterbed effect of feedback active noise control systems. *Mech. Syst. Signal Process.* **2018**, *106*, 13–23. [CrossRef]